# Precursor-Directed Control of Crystalline Type in Atmospheric Pressure CVD Growth of $TiO_2$ on Stainless Steel

Philip Evans,† Martyn E. Pemble,‡ and David W. Sheel*,†

*Institute for Materials Research, University of Salford, Salford M5 4WT, United Kingdom, and Tyndall National Institute, University College Cork, Lee Maltings, Prospect Row, Cork, Republic of Ireland*

*Received April 7, 2006. Revised Manuscript Received July 12, 2006*

Titanium dioxide thin films were grown onto stainless steel by thermal atmospheric pressure chemical vapor deposition using two different titania precursors, titanium tetraisopropoxide and titanium tetrachloride. It is demonstrated that the use of titanium isopropoxide in a nitrogen carrier gas over the temperature range 450−650 °C results in the growth of anatase at lower temperatures (450−550 °C) and a mixture of anatase and rutile at temperatures between 550 and 650 °C. In contrast, the use of $TiCl_4$ in conjunction with ethyl acetate as oxygen source in a nitrogen carrier gas over the temperature range 550−650 °C results in the exclusive growth of rutile. Below 550 °C, little or no growth was observed using $TiCl_4$/ethyl acetate. We therefore identify a structure-directing role exerted by the different precursor chemistries, which is discussed in terms of possible differences in the rates of the nucleation and growth processes taking place.

## Introduction

Titanium dioxide ($TiO_2$) thin films are chemically stable, possess a high refractive index, and have excellent transmittance in the visible and near-IR spectral regions.[1] This has therefore led to extensive applications of $TiO_2$, such as in antireflection coatings, waveguides[2] and as photocatalysts.[3]

A number of techniques have been developed for depositing titanium dioxide thin films.[4−6] Among them, atmospheric pressure chemical vapor deposition (APCVD) is one of the most attractive, as it allows close control of growth parameters (and thus of stoichiometry and microstructure), offers films that are mechanically robust and durable, and is especially applicable to large-area, continuous deposition,[7] as required for growth on glass or steel substrates where. in some cases. high volumes are desirable. In comparison to coating on glass, the coating of steels with $TiO_2$ and related materials is still in its infancy. The polycrystalline structure of stainless steel, compared to the amorphous nature of glass, may offer new possibilities in terms fo thin film properties and large-scale exploitation.

Titanium dioxide exhibits three major crystal phases as naturally occurring materials. These are rutile, anatase, and brookite.[8] In nature, rutile is the most common crystal phase, and brookite the rarest. Other structures do exist, such as cotunnite $TiO_2$, which is synthesized at high pressure and is one of the hardest oxide materials known.[9] However, only anatase and rutile play any role in the main applications of titanium dioxide. Most commonly, the form used in semiconductor photocatalysis is anatase as this is generally reported as being the most active[10] and easiest to produce of the three. Rutile is the most interesting in terms of optical applications, having the highest refractive index of the two (2.61−2.90).[11] It is also the most thermodynamically stable form.

Titania has received increasing attention in recent years due to the large-scale commercialization of self-cleaning glazing products. These products utilize titania as a photocatalyst to provide self-cleaning properties. Utilizing stainless steel as the substrate for titania film growth opens up many more potential applications because of its physical properties. Potential applications include self-cleaning surfaces for use in architecture and construction. The shape-forming properties of stainless steel also lend it to many further applications that may utilize another property of photocatalytic titania, its ability to be used as an antimicrobial coating.[12] These could include self-cleaning/sterilizing hospital equipment and

* Corresponding author. E-mail d.w.sheel@salford.ac.uk.
† University of Salford.
‡ University College Cork.

(1) Caiteanua, D.; Györgya, E.; Grigorescua, S.; Mihailescua, I. N.; Prodanb, G.; Ciupinab, V. *Appl. Surf. Sci.* **2006**, in press.
(2) Nishimura, S.; Shishido, A.; Abrams, N.; Mallouk, T. E. *Appl. Phys. Lett.* **2002**, *81*, 4532.
(3) Mills, N.; Elliott, I.; Parkin, S.; O'Neill, R. J.; Clark, J. *Photochem. Photobiol., A* **2002**, *151*, 171.
(4) Zhang, J.-Y.; Boyd, I. W.; O'Sullivan, B. J.; Hurley, P. K.; Kelly, P. V.; Senateur, J.-P. *J. Non-Cryst. Solids* **2002**, *303*, 134.
(5) Ohko, Y.; Saitoh, S.; Tatsuma, T.; Fujishima, A. *J. Electrochem. Soc.* **2001**, *148*, B25.
(6) Fernandez, A.; Lassaletta, G.; Jimenez, V. M.; Justo, A.; Gonzalez-Elipe, A. R.; Herrman, J.-M.; Tahiri, H.; Ait-Ichou, Y. *Appl. Catal., B* **1995**, *7*, 49.
(7) Pemble, M. E.; Sheel, D. W. *CVD Coatings on Glass*; 4th International Conference on Coatings on Glass, Braunschweig, Germany, Nov 3−7, 2002.
(8) Moret, M. P.; Zallen, R.; Vijay, D. P.; Desu, S. B. *Thin Solid Films* **2000**, *366*, 8.
(9) Dubrovinsky, L. S.; Dubrovinskaia, N. A.; Swamy, V.; Muscat, J.; Harrison, N. M.; Ahuja, R.; Holm, B.; Johansson, B. *Nature* **2001**, *410*, 653.
(10) Aminian, M. Kh.; Taghavinia, N.; Iraji-zad, A.; Mahdavi, S. M.; Chavoshi, M.; Ahmadia, S. *Nanotechnology* **2006**, *17*, 520.
(11) Hitchman, M. L.; Alexandrov, S. E. *Electrochem. Soc. Interface* **2001**, *10*, 40.
(12) Amézaga-Madrid, P.; Nevárez-Moorillón, G. V.; Orrantia-Borunda, E.; Miki-Yoshida, M. *FEMS Microbiol. Lett.* **2002**, *211*, 183−188.

10.1021/cm060816k CCC: $33.50 © 2006 American Chemical Society
Published on Web 11/07/2006

antimicrobial coatings for inclusion in air-conditioning units or kitchen appliances.

Despite there already being a number of publications aimed at studying thin films of titanium dioxide on glass, only a handful of publications have been produced in which stainless steel has been utilized as the substrate. Zhu et al. used the sol−gel method to deposit thin films of titanium dioxide from titanium *tert*-butoxide; these films were found to be exclusively anatase.[13] Battiston et al. used LP-MOCVD to deposit titanium dioxide using titanium tetraisopropoxide (TTIP) on a range of substrates that included stainless steel; again, all films were anatase, with rutile being achievable only by postdeposition annealing at temperatures >900 °*C*.[14] The authors found only one article in which APCVD had been utilized to deposit titanium dioxide thin films onto stainless steel. Duminica et al. utilized APCVD to deposit titanium dioxide onto stainless steel using TTIP.[15]

In our work, we have studied the growth of $TiO_2$ on stainless steel from the perspective of the potential application of such coatings as protective, self-cleaning, or antibacterial coatings. In this paper, we report for the first time the deposition of titanium dioxide onto stainless steel using titanium (IV) chloride ($TiCl_4$) in combination with ethyl acetate. We have also studied films grown using titanium isopropoxide (TTIP) and demonstrate the clear differences in the resulting films arising from a structure-directing role played by the precursors. Possible explanations of this structure-directing role are examined.

## Experimental Section

All CVD investigations were carried out using a horizontal cold wall APCVD quartz reactor. The titania thin films were deposited onto stainless steel 304L substrates of dimensions (160 × 60 mm, 0.75 mm thickness). The stainless steel substrates were cleaned prior to use by washing with warm water and detergent, then rinsing with water, isopropanol, and finally distilled water, before being dried in air. The substrates were heated on a graphite block containing three cartridge heaters (Watlow, 1.6kW). All gas lines were made of stainless steel (1/4″ O.D.) and were heated to prevent precursor condensation and ensure temperature reproducibility.

The precursors were delivered via bubblers of stainless steel construction. The bubblers were placed in aluminum jackets mounted on hotplates, so as to ensure even temperature distribution. The titanium tetraisopropoxide (Aldrich, 97%) was heated to 110 °C and added to the gas stream using preheated nitrogen (1.0 L $min^{-1}$), whereas the total gas flow to the reactor was 11 L $min^{-1}$ (no additional oxygen was used). The titanium tetrachloride (Aldrich, 99.9%) was heated in the same bubbler configuration to 68 °C and was delivered to the gas stream using a 0.2 L $min^{-1}$ flow of preheated nitrogen. The oxygen source for this work, ethyl acetate (Aldrich, 99.8%), was heated to 42 °C and delivered using preheated nitrogen.

For both precursors, a range of films were grown, so as to vary film thickness and deposition temperature. Film thickness was controlled directly by deposition time. The deposition temperature was varied from 450 to 650 °C for TTIP film growth and from 550 to 650 °C for $TiCl_4$.

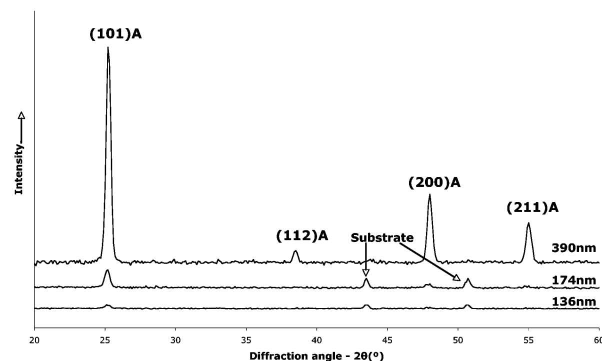


**Figure 1.** XRD patterns of $TiO_2$ films of 136, 174, and 390 nm deposited on stainless steel using TTIP.

X-ray diffraction measurements were performed using a Siemens D5000 diffractometer under specific operating conditions: 40 kV, 40 mA, 2$\theta$ 20.0−60.0°, step size 0.1°, and time 30 s per degree, with a glancing angle of 2°. All peak positions and diffraction intensities were matched with database spectra. Raman spectrometry was performed using a Renishaw 1000 spectrometer at a 514 nm wavelength. The surface morphology was investigated using scanning electron microscopy (Philips XL30 FEGSEM). X-ray photoelectron spectroscopy was performed on a Thermo VG Scientific spectrometer using aluminum radiation.

## Results

**TTIP Film Growth.** The crystallinity of the films was evaluated separately as a function of varying thickness (at fixed deposition temperature) and varying deposition temperature (using a similar thickness). For the purpose of making reliable measurements of film properties as a function of thickness, a deposition temperature of 500 °C was selected, because at this temperature, highly uniform films could be grown. It was found that at this temperature, all films were anatase, such that the crystalline type was independent of thickness, Figure 1. Figure 1 also shows that, in general, the preferred orientation of the films was toward (101).

From Figure 1, it may be seen that for the thinner films (<300 nm), peaks corresponding to the substrate were detected at 44.3 and 50.7° because of the low incidence angle that was necessary to improve peak intensity. Upon the film thickness being increased, more anatase reflections were observed, although the (101) peak remains the most intense.

Using TTIP, it was possible to deposit films from 450 to 650 °C. For deposition in the temperature range 450−500 °C, anatase was exclusively observed as the titanium dioxide phase present. At 550 and 650 °C, mixtures of anatase and rutile were observed with weight anatase fractions of 59.9 and 53.2%, respectively. The anatase weight fraction was calculated using the Spur and Myers method.[16] The occurrence of a significant proportion of rutile at these relatively low temperatures is of interest and suggests that the substrate has a direct influence on the nucleation and growth processes. The mean crystallite size was calculated from the fwhm of the anatase (101) peaks using Scherrer's formula.[17] Figure

(13) Zhu, Y.; Zhang, L.; Wang, L.; Fu, Y.; Cao, L. *J. Mater. Chem.* **2001**, *11*, 1864.
(14) Battison, G. A.; Gerbasi, R.; Porchia, M. *Thin Solid Films* **1994**, *239*, 186.
(15) Duminica, F.-D.; Maury, F.; Senocq, F. *Surf. Coat. Technol.* **2004**, *188−189*, 255.
(16) Spurs, R. A.; Myers, H. *Anal. Chem.* **1957**, *29*, 760.
(17) Cullity, B. D. *Elements of X-Ray Diffraction*; Prentice Hall: Upper Saddle River, NJ 2001.

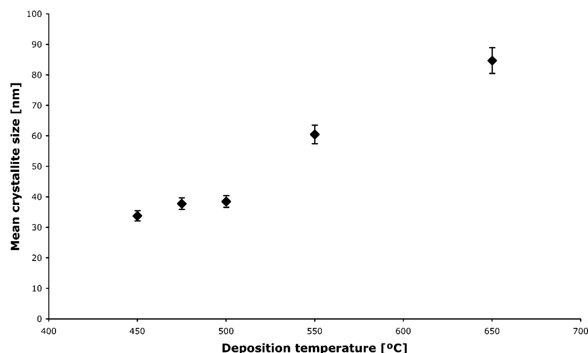


**Figure 2.** Graph to show anatase (101) mean crystallite size variation as a function of deposition temperature in $TiO_2$ films, as determined by the Scherrer formula[17].

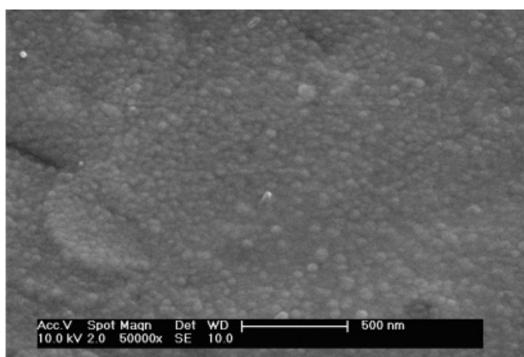


118nm

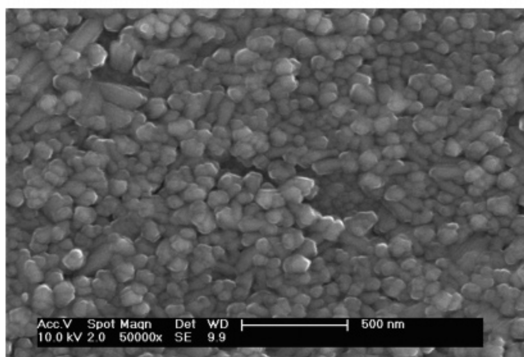


299nm

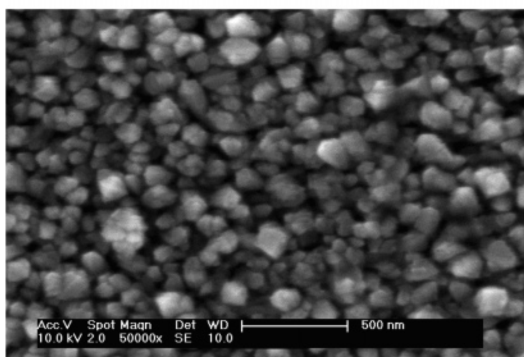


465nm

**Figure 3.** SEM images of $TiO_2$ films deposited at 500 °C using TTIP.

2 shows the mean crystallite size calculated as a function of deposition temperature between 450 and 650 °C.

SEM experiments were performed in order to study the morphology of the films, Figure 3. It was observed that thinner films deposited at 500 °C were denser and exhibited a narrow particle size distribution with an average particle size of 26 nm (standard deviation 4 nm) for the 118 nm film. As film thickness increased, the surface appeared less dense with growth at specific sites, suggestive of a Stranski−Krastanov type of growth mechanism.[18]

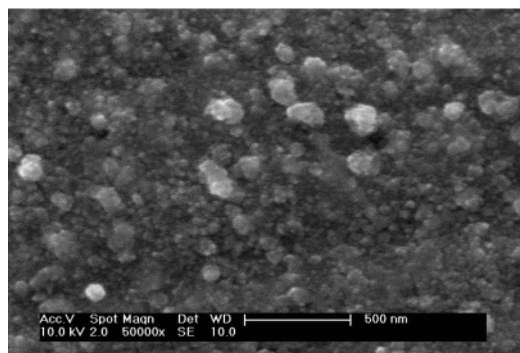


550°C

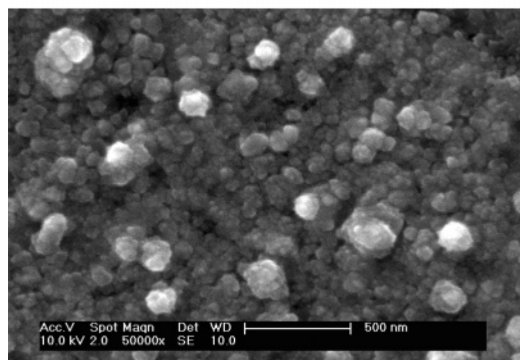


650°C

**Figure 4.** $TiO_2$ film (157 nm) deposited using TTIP at 550 and 650 °C.

When films of comparable thickness deposited at different temperatures were examined, it appeared that films grown at temperatures up to 500 °C were relatively homogeneous and that particle size increased slightly with increasing deposition temperature. For growth at 550 and 650 °C, there was proposed evidence of gas-phase nucleated particles in the SEM images (Figure 4) with increasing deposition temperature. The gas-phase nucleated particles are suggested to be clusters on the surface that are accompanied by a visible increase in haze, eventually leading to a white powder on the surface. This dramatic change in change in growth mechanism, from a surface-phase dominated reaction to one dominated by gas-phase reactions, might account for the appearance of rutile at these temperatures.

All of the films grown using TTIP showed good or excellent adhesion. The films deposited at 450−500 °C showed excellent adhesion and passed the Scotch Tape test with no visible degradation. A coated sample was bent through 180°, and then bent back flat, again with no visible signs of degradation or peeling of the films. At 550 and 650 °C, gas-phase nucleation was observed. This manifested itself visually as hazy or powdered deposits on the surface. Some of the powder could be removed by the Scotch Tape test; however, a well-adhered layer remained that also showed the same excellent adhesion of the samples deposited at 450−500 °C.

(18) Ohring, M. *The Materials Science of Thin Films*; Academic Press: London, 1992.

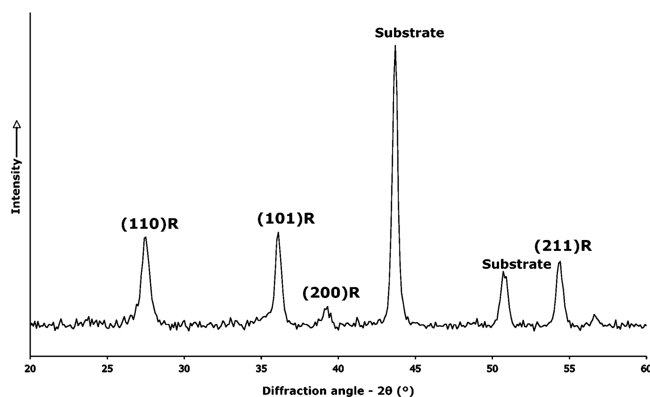


**Figure 5.** XRD pattern of a 146 nm $TiO_2$ film deposited using $TiCl_4$ and ethyl acetate at 650 °C.

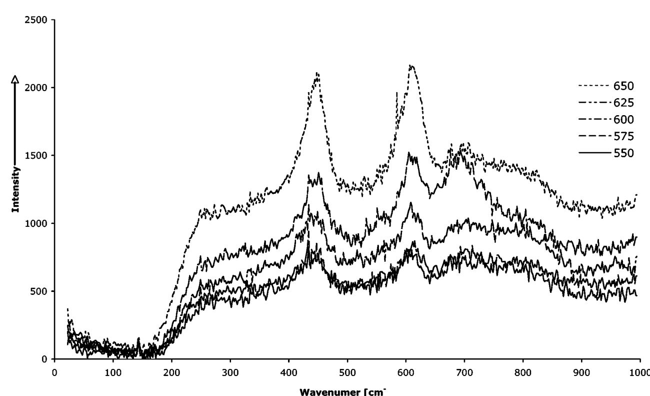


**Figure 6.** Raman spectra of $TiO_2$ films deposited using $TiCl_4$ in the temperature range 550−650 °C showing rutile peaks.

**$TiCl_4$ and Ethyl Acetate Film Growth.** In contrast to the films grown using TTIP, those films grown using titanium tetrachloride and ethyl acetate were found to be exclusively the rutile phase of titanium dioxide; regardless of thickness or deposition temperature (550−650 °C). Figure 5 shows the XRD patterns of films of different thickness. Substrate peaks were also observed in the thinner films.

The Raman spectra in Figure 6 represent films of similar thickness deposited at different temperatures. Films deposited between 550 and 650 °C displayed two peaks, at 446[1] and 610 $cm^{-1}$. These are characteristic of the rutile structure and their position is in agreement with literature values to within ±1 $cm^{-1}$.[19] There is an additional peak at around 700 $cm^{-1}$ on the spectra; a similar peak has been observed on a substrate that had been heated in the reactor but was uncoated, where it was attributed to a mix of iron and chromium oxides.[20] Thus, the peak at ~700 $cm^{-1}$ could be due to detection of the substrate. However, given the thickness of the film, it seems unlikely that such a peak could be detected using Raman. Thus, it is also possible that the peak arises from iron and chromium oxides species, which have somehow been transported either into the $TiO_2$ layer or through the layer surface.

Busca et al. have reported a fwhm increase from 20 $cm^{-1}$ to 30 $cm^{-1}$ which they observed when the crystallite size decreased from 50 nm to 9 nm.[21] In Figure 6 the fwhm of the peak at 446 $cm^{-1}$ for the spectra corresponding to the films grown at 650 °C and 550 °C increases from 38 ± 1$cm^{-1}$ to 55 ± 1$cm^{-1}$ respectively. Thus by comparison with the work of Busca et al., it is suggested that in the experiments performed here, the crystallite size in $TiCl_4$ films decreases with decreasing deposition temperature, although other factors may also have a significant influence on the fwhm.

From the SEM images in Figure 7, it can be seen that the thinnest film appears the most dense, has the smallest particle size, and is the most homogeneous. As the film thickness increases, the particle size increases, with preferential growth on specific sites making the surface appear rougher. The thicker films appear less dense because of growth at specific sites, such that the underlying particles that would have been foremost if the film were thinner can be observed in the gaps between the larger particles. Similarly to the films grown using TTIP, this initial (monolayer) growth followed by specific site growth is very suggestive of a Stranski−Krastanov type growth mechanism.

However, the most distinctive feature in Figure 7 is the particle shape. For the two thickest films, these were not rounded in shape (like those formed from TTIP), but exhibited an increasingly well-defined blocklike structure with increasing film thickness. It is likely that the occurrence of such particle shapes is related to the rutile structures observed in the $TiCl_4$ films. This transformation in particle shape shows that the effect of altering the precursor chemistry is quite remarkable and suggests that different film nucleation and growth characteristics may be imparted by the choice of precursor chemistry.

All of the films deposited using $TiCl_4$ showed excellent adhesion. They showed no signs of degradation using the Scotch Tape test. Coated samples could be bent through 180° with no visible degradation and the film remaining intact.

**Characterization of the Photocatalytic Activities of the Titania Films.** The photocatalytic activities of a number of the titanium dioxide films were measured by studying the rate of degradation of stearic acid under UV radiation. The integrated area of the C−H stretching peaks (2800−3000 $cm^{-1}$) was measured using FT-IR and plotted as a function of timed exposure to 3 mW $cm^{-2}$ UV radiation; the photocatalytic activity was determined by the gradient of this line. The photocatalytic activity for the titania films grown by TTIP and $TiCl_4$ were found to be $7.6 \times 10^{-4}$ $cm^{-1}$ $min^{-1}$ and $9.0 \times 10^{-5}$ $cm^{-1}$ $min^{-1}$, respectively. The anatase TTIP film was more active than the rutile $TiCl_4$ film, which has been reported previously.[22] However, both films were less active when compared to the photocatalytic activity of a commercially available self-cleaning glass product ($9 \times 10^{-3}$ $cm^{-1}$ $min^{-1}$). Iron and chromium were detected in depth profiles of both the TTIP and TiCl4 films; it is quite likely that these heterocations act as electron−hole recombination

(19) Zhang, Y.-H.; Chan, C. K.; Porter, J. F.; Guo, W. *J. Mater. Res.* **1998**, *13*, 2602.

(20) *The Raman Spectra Database of Minerals and Inorganic Material (RASMIN)*, updated Dec 2004, accessed via http://www.aist.go.jp/RIODB/rasmin/E-index.htm, last accessed May 14, 2005.

(21) Busca, G.; Ramis, G.; Amores, J. M. G.; Escribano, V. S.; Piaggio, P. *J. Chem. Soc., Faraday Trans.* **1994**, 3181

(22) Sclafani, J. M.; Herrmann, *J. Phys. Chem.* **1996**, *100*, 13655−13661.

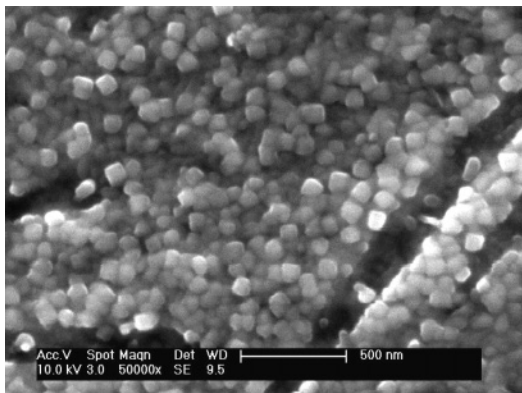


127nm

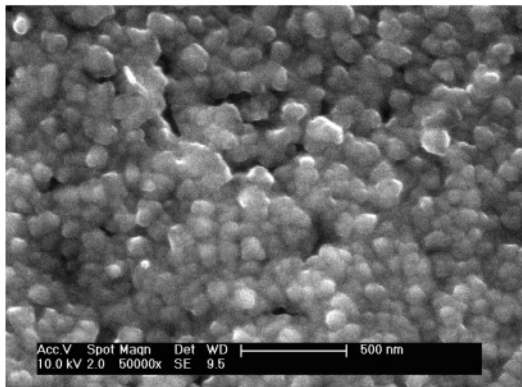


164nm

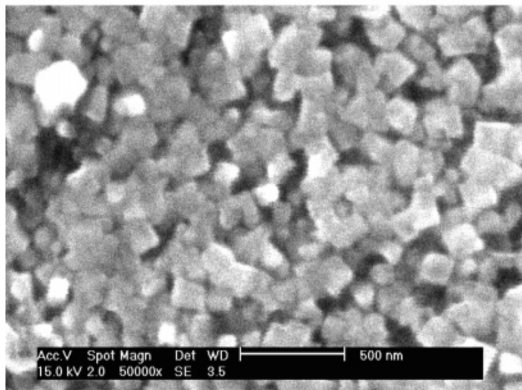


281nm

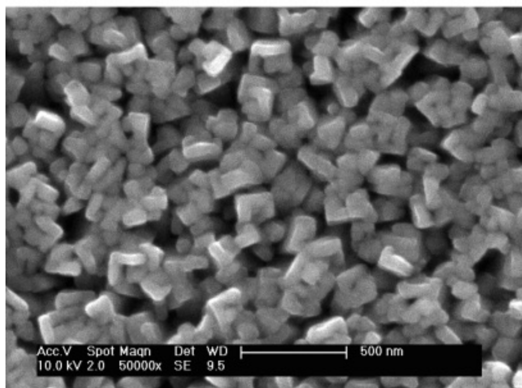


366nm

**Figure 7.** SEM images of $TiO_2$ films grown from $TiCl_4$ and ethyl acetate at 650 °C.

centers and consequentially reduce the photoactivity of the films.[23]

**Scheme 1. Reaction of TTIP to $TiO_2$ via an Intramolecular Reaction**

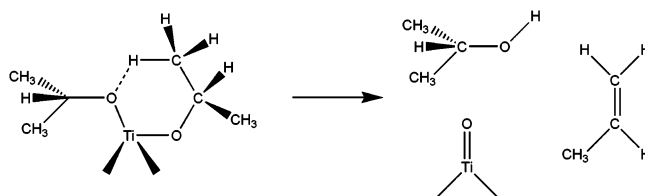

## Discussion

**Structure Directing Role of the Titania Precursors.** The reaction mechanism for the formation of $TiO_2$ from titanium alkoxides has been extensively studied in the literature. Scheme 1 shows how, via an intramolecular reaction (which is then repeated), it is possible to produce $TiO_2$ directly from TTIP.

Further support for an intramolecular mechanism also comes from the observation that $TiO_2$ nanoparticles may be formed directly from the reaction of TTIP in the gas phase,[24] whereas surface studies have interpreted the formation of $TiO_2$ on Si (100) from TTIP as arising from the stepwise decomposition of TTIP along the lines of the processes depicted in Scheme 1, i.e., the Si (100) surface simply acts as a support for what is otherwise intramolecular chemistry.[25] Intermolecular reactions involving water, propene, and acetone can also occur.[26]

In contrast, the reaction between $TiCl_4$ and ethyl acetate has been little studied; no direct references to the reaction mechanism between $TiCl_4$ and ethyl acetate could be found in the literature. $TiCl_4$ has no on-board source of oxygen; therefore, the reaction leading to $TiO_2$ formation must be an intermolecular one. In the context of producing $TiO_2$ from $TiCl_4$, ethyl acetate is a more controllable oxygen source when compared to the simple hydrolysis reaction that is observed between $TiCl_4$ and water. (It therefore fits with our observations that the film growth for the $TiCl_4$ films was slower than the films grown from TTIP.)

In this respect, it could be suggested that the ethyl acetate needs to react to produce oxidant species in situ and at the deposition temperatures used in these experiments, it is likely that the ethyl acetate decomposes. Possible decomposition routes would result in the formation of acetic acid via the $\beta$-hydrogen elimination of ethene, or decomposition to form ketene and ethanol. At the deposition temperatures employed in this work, ethanol could subsequently dehydrate to evolve water and ethane; the reaction could then proceed via a simple hydrolysis reaction, essentially rendering the ethyl acetate as a masked water precursor.

Alternatively, in the presence of $TiCl_4$, direct concerted attack of the ethoxy oxygen (on the ethyl acetate) at a Ti center can result in the substitution of a Cl atom by an ethoxy group, with the subsequent elimination of acetyl chloride.

(23) Litter, M. I.; Navio, J. A. *J. Photochem. Photobiol., A* **1996**, *98*, 171–181.
(24) Backman, U.; Auvinen, A.; Jokiniemi, J. K. *Surf. Coat. Technol.* **2005**, *192*, 81.
(25) Cho, S.-I.; Chung, C.-H.; Moon, S. H. *J. Electrochem. Soc.* **2001**, *148*, C599.
(26) Wu, Y.-M.; Bradley, D. C.; Nix, R. M. *Appl. Surf. Sci.* **1993**, *64*, 21–28.

Although at this stage it is speculative to predict differences in reaction rates for equivalent growth temperatures based on postulated mechanistic descriptions, it seems reasonable to propose that the observed differences in structure are related to the inherently slower growth rate of $TiCl_4$ and ethyl acetate compared to growth with TTIP. Han et al. recently reported that the control of the reaction rate is a key factor in obtaining $TiO_2$ nanocrystals with the desired crystalline structure and/or shape,[27] a fact that is evident in the SEM images of our films (see Figures 3 and 7). The choice of precursor chemistry had a notable effect on the resulting particle shape, and a slower growth rate would allow for the growth that would be required to form the blocklike structures observed in our $TiCl_4$ grown films. Han et al. provide further evidence to support to our observations in that they reported the growth of rutile nanoparticles from TTIP when HCl was included in their reaction conditions, whereas anatase was detected with NaCl or acetic acid addition. It is very likely that some HCl is formed during the reaction between $TiCl_4$ and ethyl acetate, and thus a similar interaction as seen by Han et al. may be taking place here.

Also in this respect, Hitchman et al. have shown that rutile may be deposited exclusively at very low temperatures (ca. 300 °C) from tetraisobutyl titanium, and although these workers did not produce a rigorous explanation for this observation, it was noted that growth took place slowly when using the particular precursor concerned, as compared to the use of TTIP.[28] One reason for this could be the fact that the hydrolysis of the alkoxide is the key step to obtaining $TiO_2$, and that the ease with which titanium alkoxides are hydrolyzed decreases with increasing chain length.[29]

Thus it may be that under our reaction conditions, perhaps in this case also aided by the particular crystalline conditions present on a stainless steel surface and possibly the presence of HCl, slow film growth essentially favors the formation of rutile, whereas faster growth permits the formation of some, or exclusively, anatase.

It is proposed that this phenomenon would not simply be explainable in terms of the relative thermodynamic stabilities of anatase and rutile. Many workers have studied the thermally driven anatase to rutile phase transition.[10] In general, this is found to be a complex phenomenon, particularly where nanocrystalline $TiO_2$ particles are involved.[19] Because growth rate and particle size are linked parameters, it would not be unreasonable to suggest that for film growth, the same considerations would apply.

## Conclusions

In summary, we have demonstrated that polycrystalline titania can be deposited onto stainless steel by thermal APCVD. The phase of the titania films can be controlled by careful selection of precursor and experimental conditions. Films grown using titanium tetraisopropoxide (TTIP) were anatase, whereas films grown using titanium tetrachloride ($TiCl_4$) were rutile. The mean crystallite size of the films increased with increasing film thickness. An explanation for the difference in phase resulting from the different precursors has been discussed in terms of the nucleation and growth rate of the films, which was faster for the TTIP than the $TiCl_4$ films, and in terms of possible reaction mechanisms.

**Acknowledgment.** The authors gratefully acknowledge the support of Dr. T. English and Dr. D. Hammond of Corus plc for their support, and the Engineering and Physical Sciences Research Council.

CM060816K

(27) Han, S.; Choi, S-H.; Kim, S.-S.; Cho, M.; Jang, B.; Kim, D.-Y.; Yoon, J.; Hyeon, T. *Small* **2005**, *1*, 812.
(28) Hitchman, M. L.; Zhao, J. *J. Phys. IV France* **1999**, *9*, Pr8−357.
(29) Cotton, F. A.; Wilkinson, G.; Murillo, C. A.; Bochmann, M. *Advanced Inorganic Chemistry,* 6th ed.; Wiley: New York, 1990; p 702.